

# ZnO-Incorporated ZSM-5 for Photocatalytic CO<sub>2</sub> Reduction into Solar Fuels under UV/Visible Light

Adhi Satriyatama<sup>1</sup>, Ignatius Dozy Mahatmanto Budi<sup>1</sup>, Hilya Nadhira Iman<sup>1</sup>, Henry Susilo<sup>1</sup>, and Wibawa Hendra Saputera<sup>1\*</sup>

<sup>1</sup> Department of Chemical Engineering, Faculty of Industrial Technology, Institut Teknologi Bandung, Jl. Ganesha No. 10, Bandung 40132, Indonesia; adhisatriyatama@students.itb.ac.id; ignatiusdozy@students.itb.ac.id; hilyanadhira@students.itb.ac.id; henrysusilo@students.itb.ac.id.

\* Correspondence: hendra@che.itb.ac.id

**Abstract:** Direct conversion of CO<sub>2</sub> into chemical compounds become a prospective pathway to transform CO<sub>2</sub> into valuable chemical compounds. Introduction of porous materials with high uptake into the photocatalytic system can enrich the CO<sub>2</sub> absorption on the surface of the photocatalyst for catalytic conversion. In this regard, another feasible strategy can be accomplished via combining commercial photocatalyst material into porous supporting materials. The present study investigated a series of ZnO-incorporated ZSM-5 catalysts to produce solar fuels under UV/Visible light irradiation. ZnO/ZSM-5 was synthesized using wet-impregnation method using Zn(CH<sub>3</sub>COO)<sub>2</sub> as reagent and followed by calcination. Various characterizations were also conducted to study the morphology, structure, absorbance, and physiochemical properties of photocatalyst. SEM-EDX images showed that ZnO was successfully incorporated into ZSM-5 surfaces with particle size around 50 nm. Optical properties of the ZnO/ZSM-5 corresponds to 3.36 eV, showing the increase of the band gap value than pure ZnO, which corresponds to 3.18 eV. The solar fuels production including formic acid (HCOOH), formaldehyde (HCHO), and methanol (CH<sub>3</sub>OH) evolution was evaluated under UV/Visible irradiation. The design composite ZnO/ZSM-5 catalyst achieves a methanol and formic acid yields of 39.2 μmol/g.h and 0.72 μmol/g.h μmol/(g.h), respectively which exhibit about 1.5 and 2.5-folds higher compared to neat ZnO catalyst. The improved yield and selectivity towards methanol product is attributed to the greater light-absorption, more efficient charge transfer, nanostructure morphology, and more active sites available for the CO<sub>2</sub> adsorption.

**Keywords:** ZnO, zeolite, ZSM-5, wet-impregnation, CO<sub>2</sub> utilization, photocatalysis

**Citation:** Satriyatama, A.; Budi, I.D.M.; Iman, H.N.; Susilo, H.; Saputera, W.H. ZnO-incorporated ZSM-5 for photocatalytic CO<sub>2</sub> reduction into solar fuels under UV/Visible light. *Chem. Proc.* **2021**, *3*, x. <https://doi.org/10.3390/xxxxx>

Published: 20 October 2021

**Publisher's Note:** MDPI stays neutral with regard to jurisdictional claims in published maps and institutional affiliations.



**Copyright:** © 2021 by the authors. Submitted for possible open access publication under the terms and conditions of the Creative Commons Attribution (CC BY) license (<https://creativecommons.org/licenses/by/4.0/>).

## 1. Introduction

In recent years, CO<sub>2</sub> conversion into valuable chemicals, such as CH<sub>3</sub>OH, H<sub>2</sub>CO, HCOOH, CO, and CH<sub>4</sub> via photocatalysis is presented as alternative technology in overcoming the current global emission [1,2]. The design of photocatalyst materials become the major challenges, particularly to produce highly active and selective product. Among various photocatalysts, zinc oxide (ZnO) is one of the widely investigated due to its high photoactivity, highly chemical and thermal stability, low cost, and non-toxicity [3,4]. However, the applications of ZnO are heavily limited by the wide range of bandgap ( $E_g = 3.27$  eV), rapid recombination, poor solar light utilization, and photochemical corrosion. Moreover, ZnO particles also can easily agglomerate, which led to worse performance in industrial application [5].

Therefore, many different approaches have been adopted to overcome the disadvantage of pristine ZnO, which mainly focused to improve the specific surface area and more reaction active sites in order to enhance the photocatalytic activity [6]. From this point, another feasible approach can be accomplished via combination of ZnO with

other inorganic porous materials, like graphene oxide [7], single-walled carbon nanotubes [8], fullerenes [9], and Pd [10], which successfully improved its photocatalytic activity. For this purpose, zeolite is considered as a good candidate to perform as a support of photocatalysts. The porous structure of zeolite was able to confine small molecules such as CO<sub>2</sub> to further enhance its photocatalytic activity. Moreover, zeolite has been applied as supporting material for various hetero-structured photocatalyst, like TiO<sub>2</sub>/Clinoptilolite [11], Ag-TiO<sub>2</sub>/Zeolite-Y [12], ZnO/Zeolite-Y [13], and SnO<sub>2</sub>/Clinoptilolite [14]. However, these reported works mainly focused on air and pollutant degradation which exhibited higher efficiency compared to bare materials. Among different type of zeolites, ZSM-5 zeolite is considered as the most widely applied materials as catalyst supports, due to its high surface area, surface acidity, ion-exchange capacity, strong adsorption, and chemical stability [15,16]. It also important to note that immobilization of metal oxide over ZSM-5 zeolite in well-dispersed form can affect the increased bandgap energy as well as decreased rate of electron-hole recombination [16,17].

In this study, zinc acetate (Zn(CH<sub>3</sub>COO)<sub>2</sub>) was used as Zn sources, to prepare ZnO/ZSM-5 photocatalyst via a wet-impregnation method. The crystal structure, functional group, morphology, and pore structure of the samples were characterized by X-ray diffraction (XRD), Fourier Transform Infrared (FTIR), scanning electron microscopy (SEM), diffuse reflectance ultraviolet-visible spectrometry (DRUV-Vis), and N<sub>2</sub> adsorption/desorption and pore size distribution analysis, respectively. The product yield and selectivity were also investigated.

## 2. Materials and Methods

### 2.1. Materials

ZSM-5 (provided by Meiqi Industry & Trade Co Ltd., China) was used as the catalyst support in all experiments. Chemicals were analytical grade and used as supplied: Zn(CH<sub>3</sub>COO)<sub>2</sub>·2H<sub>2</sub>O (>99%, Merck) and ZnO (>99%, Sigma-Aldrich®).

### 2.2. ZnO/ZSM-5 Synthesis

Impregnation method was used to synthesize ZnO/ZSM-5 as reported in the previous literature [18]. The concentration of Zn(CH<sub>3</sub>COO)<sub>2</sub>·2H<sub>2</sub>O was matched to obtain 5%-wt of ZnO content. Then, a suitable amount commercial ZSM-5 powder was dispersed in the mixture. The mixtures were stirred for 24 h. The slurry was then dried at 110 °C for 6 h. Calcination was performed at 350 °C under N<sub>2</sub> gas flow with heating flow rates of 5 °C/min for 5 h.

### 2.3. ZnO/ZSM-5 Characterization

X-ray diffractometer (Shimadzu, Tokyo, Japan) was used to analyze the crystallography profile of the samples. The morphology was observed by SEM (JEOL JSM-6510LA (JEOL Company, Musashino, Tokyo, Japan)). The light response and bandgap of the samples were evaluated by dual-beam UV-Vis diffuse reflectance spectrophotometer (Shimadzu, Tokyo, Japan). The N<sub>2</sub> adsorption-desorption isotherms of the samples were measured using a Quantachrome Nova 4200E (Kanagawa, Japan) equipment. The FTIR instrument (PerkinElmer) was used to investigate the functional group in the range wave-number of 500-3750 cm<sup>-1</sup>.

### 2.4. Photocatalytic Activity Assessment

The photocatalytic reduction of CO<sub>2</sub> into solar fuels was measured in a photoreaction system under UV-vis light irradiation (λ = 300–1100 nm) emitted from a 300 W Xe lamp. Before the mixture was added to the reactor, the as-prepared sample (1 g/L) was dispersed in the deionized water (400 mL) with continuous mixing for 30 minutes. The photoreaction system was purged with the high-purity nitrogen for 30 minutes before turning on the lamp. The temperature and pressure of reactor was controlled at room temperature and ambient condition, respectively. The final products were analyzed after 4 hours of reaction using a gas chromatography equipped with a thermal conductivity detector

(TCD) for gas product and high-performance liquid chromatography (HPLC) for liquid product.

### 3.1. Photocatalyst Characterization

#### 3.1.1. Structural Analysis

The crystal structure of the bare and synthesized material was investigated by X-ray powder diffraction. Figure 1a depicts the diffractograms patterns of neat ZnO, ZSM-5, and ZnO/ZSM-5. A glance at the XRD patterns reveals that impregnated samples display ZnO and ZSM-5 peaks. The presence of ZSM-5 can be confirmed from peaks at  $2\theta = 7.67, 8.61, 14.7, 23.1, 23.35, 23.72, \text{ and } 23.96$  (JCPDS 00-044-0002) in tetragonal phase. Moreover, the ZnO assigned to have peaks at  $2\theta = 31.89, 34.55, 36.39, 47.69, 56.77, 63.03, \text{ and } 68.22$  (JCPDS 01-076-0704) in hexagonal phase. By comparing with the bare ZnO and ZSM-5 data, it is also observed that incorporation of ZnO into ZSM-5, the peaks related to ZnO gradually decreasing, while the intensity of ZSM-5 peaks decreasing. The crystallite size and relative crystallinity of ZnO/ZSM-5 was 11.53 nm and 79% respectively, as it shown on the Table 1.

Figure 1b presented the FTIR spectra of ZnO/ZSM-5 in wavenumber ranged of  $400\text{--}4,000\text{ cm}^{-1}$ . As it shown from the graph, the FTIR patterns of ZnO/ZSM-5 have a similar trend with bare ZSM-5 and exposed no important change. The interacting O-H or bridging O-H groups can be observed from wide peaks at  $3,616 \text{ and } 1,551\text{ cm}^{-1}$  [42, 43]. Catalysts also possess water absorption properties from the air, which can be seen from other recorded peak at  $1,551\text{ cm}^{-1}$  [19]. Moreover, the wide peaks in the range of  $400\text{--}1,200\text{ cm}^{-1}$  wavenumber are corresponded to the Si-O(Si) and Si-O(Al) vibration in tetrahedral or alumina and silica-oxygen bridges, respectively [20]. Furthermore, the stretching vibration of Zn-O can be attributed with the peak in the range of  $400\text{--}500\text{ cm}^{-1}$  where they can also attribute to overlap peak with Zn-O bond at the region [21]. It is also important to note that the incorporation of transition metal oxide cation does not change the zeolite main structure zeolite which can be observed from appealed spectrums [22].

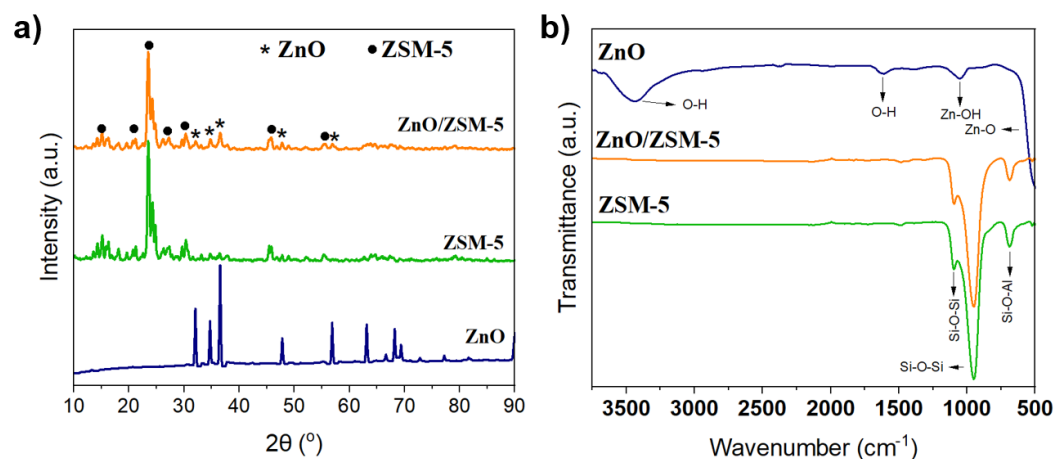


**Figure 1.** a) XRD patterns and b) FTIR spectra of ZnO, ZSM-5, and ZnO/ZSM-5.

**Table 1.** Summary of structural properties of ZnO, ZSM-5, and ZnO/ZSM-5.

Samples	Crystallite size (nm)	Relative Crystallinity (%)
ZnO	26.37	-
ZSM-5	11.53	87.53
ZnO/ZSM-5	9.94	68.33

#### 3.1.2. Morphological Analysis

Figure 2a,b presented the SEM micrographs of the samples. The morphology of ZSM-5 has a hexahedral structure, in agreement with ZSM-5 characteristics from previous reported study [23]. By incorporation ZnO into ZSM-5, the surface was covered with amount of small nano-scale ZnO particles which led to the differentiation of ZSM-5 particles. In accordance with relative crystallinity, the incorporation also affects the decreases of relative crystallinity for ZSM-5. Additionally, the grain size also changes, attributing to the electronegativity of Zn (II) in the zeolite pore structure is stronger the Si-O-Al framework [24]. This result also confirmed the irregular structure crystal grains due to the clustering phenomenon over crystal [25]. A deeper examination of the SEM results also revealed that the low amount of agglomeration is observed from the synthesized samples. Nevertheless, agglomeration is considered as the disadvantageous of excessive loading, which led to worse catalytic performance. Furthermore, these images also observed that impregnated ZnO samples catalysts have nanometric surface particles. Thus, it can provide more reactive and reducible sites as well as higher catalytic performance of the photocatalyst [26].

The SEM-EDX mapping analysis shows the existence of Al, Si, and Zn elements, which also confirmed the absence of impurities in the samples, as shown in Figure 2c. This become additional evidence that ZnO/ZSM-5 was successfully synthesized and have a well-dispersed Zn species into ZSM-5 supports. Overall, the EDX analysis results also displayed the dispersion of Zn was achieved for about 5%-wt as theoretically expected.

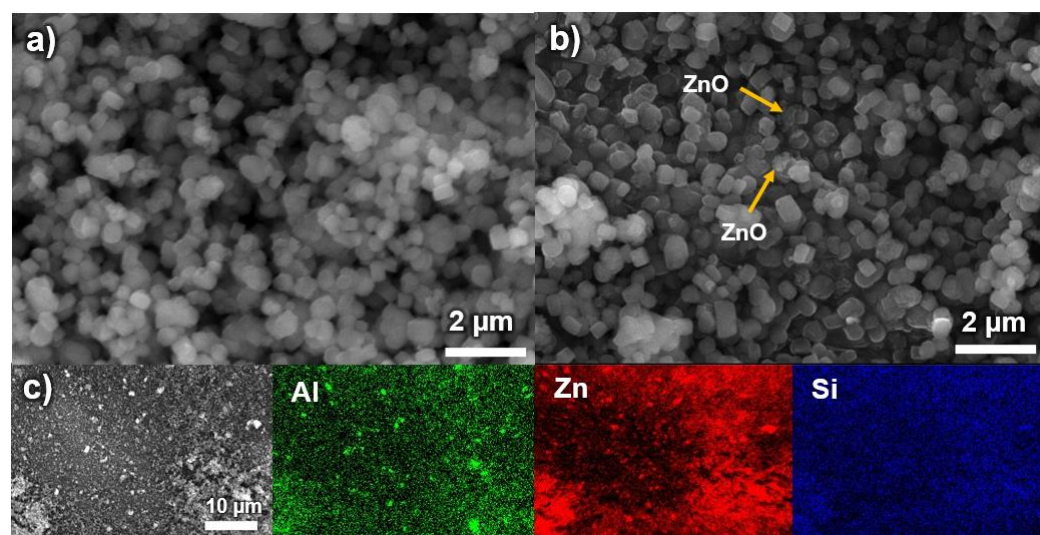


**Figure 2.** SEM morphology of a) ZSM-5, b) ZnO/ZSM-5, and c) elemental EDX mapping of ZnO/ZSM-5.

**Table 2.** Summary of elemental analysis of ZnO, ZSM-5, and ZnO/ZSM-5.

Samples	ZnO (%-wt)	Al <sub>2</sub> O <sub>3</sub> (%-wt)	SiO <sub>2</sub> (%)	Si/Al ratio
ZnO	86.12	-	-	-
ZSM-5	-	0.92	46.62	50.67
ZnO/ZSM-5	4.92	0.86	35.11	40.82

### 3.1.3. Optical Analysis

Figure 3a demonstrated the diffuse reflectance UV–visible spectra of the photocatalysts. The absorption peaks of bare ZSM-5 and ZnO are observed at 220 nm and 292 nm, respectively. The absorption peak near 292 nm may be attributed to small sub ZnO cluster, while absorption peak near 220 nm may attributed to the ZnO and ZSM-5 interaction [27]. When the ZnO content increases, the intensity of absorption peak increases gradually can be observed, which indicated that response range expanding in visible range and

photocatalytic activity improvement. Therefore, the indirect energy band gap is also narrowed based from the Tauc's plot. The band gap value of ZnO/ZSM-5 was 3.36 eV, as the blue shifts observed, as shown at Figure 3b. The shifting from red to blue shift in ZnO/ZSM-5 samples is caused by the ZSM-5 absorption in visible range (4.3 eV).

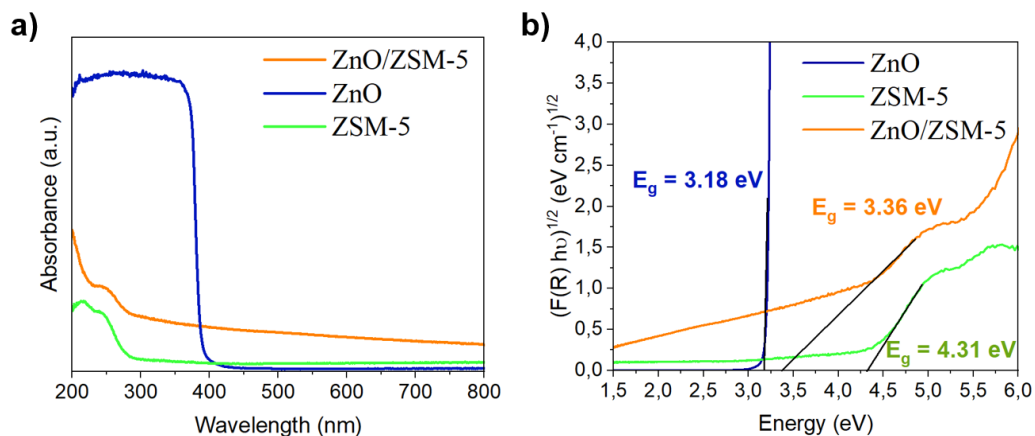


**Figure 3.** a) diffuse reflectance ultraviolet-visible spectra and b) Tauc's plot of synthesized samples.

### 3.1.4. Textural Analysis

The N<sub>2</sub> adsorption isotherm and physicochemical properties of as prepared samples is shown in the Figure 4 and Table 3. In agreement of previous studies, bare ZSM-5 and ZnO exhibited a surface area of 314.68 and 8.43 m<sup>2</sup>/g which are in the range of 300-400 m<sup>2</sup>/g and 5-40 m<sup>2</sup>/g, respectively [28,29]. Furthermore, the metal oxide loading into bare ZSM-5 decreases surface area by 1.4-folds, where it can be attributed from the deposition of zinc species into micropores. The loss of ZSM-5 crystallinity also supports this hypothesis. This results can also be justified from the agglomerations of the supported samples, which corresponded to the SEM images.

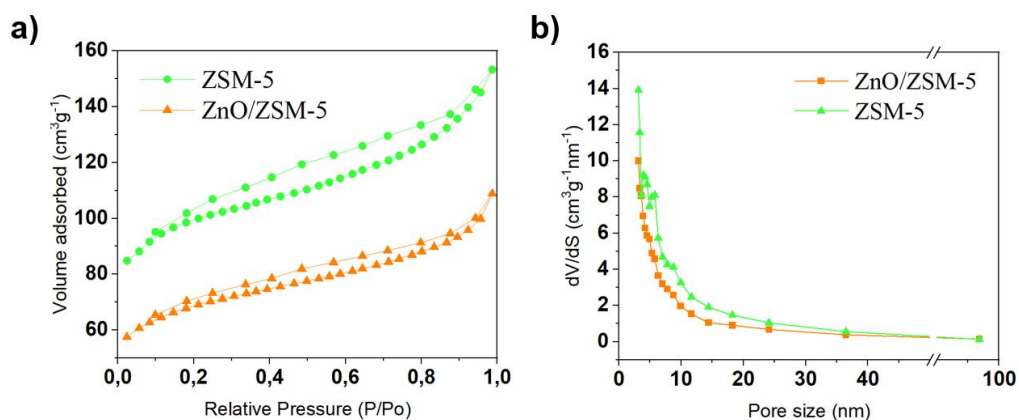


**Figure 4.** a) N<sub>2</sub> adsorption-desorption isotherms and b) pore size distribution of ZSM-5, and ZnO/ZSM-5.

**Table 3.** Summary of textural properties of ZnO, ZSM-5, and ZnO/ZSM-5.

Samples	S <sub>BET</sub> (m <sup>2</sup> /g)	Pore size (nm)	Pore volume (cm <sup>3</sup> /g)
ZnO	8.43	11.34	0.023
ZSM-5	314.68	3.05	0.178
ZnO/ZSM-5	220.49	3.02	0.237

### 3.1.5. Photocatalytic Activity

The photocatalytic performance of prepared catalysts was evaluated for CO<sub>2</sub> reduction in liquid phase under UV-visible light illumination. The obtained products including HCOOH and CH<sub>3</sub>OH were observed as shown in Figure 5. It can be seen that CH<sub>3</sub>OH was the main product of photocatalytic CO<sub>2</sub> reduction while HCOOH became the minor product when using neat ZnO and ZnO/ZSM-5 catalysts. The incorporation of ZnO into ZSM-5 exhibited remarkably photocatalytic activity reaching product yield of CH<sub>3</sub>OH and HCOOH up to 1.5 and 2.5 times higher compared to neat ZnO.

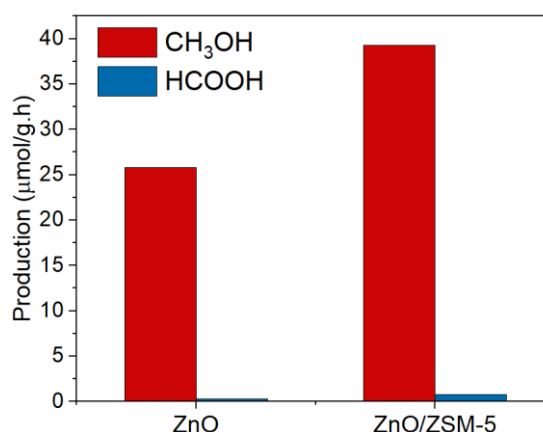


**Figure 5.** Fuel formation via CO<sub>2</sub> reduction for CH<sub>3</sub>OH and HCOOH.

The improved photocatalytic activity of ZnO/ZSM-5 can be associated with greater efficiency of charge transfer, higher surface area, and enhanced light absorption compared to neat ZnO catalyst [30]. Moreover, the presence of zeolite attributed the enhancement of CO<sub>2</sub> adsorption, as reported from the previous study under similar conditions. The adsorbed CO<sub>2</sub> become necessary as it can provide as an electron trap of numerous electrons to further generate light hydrocarbon products. Ultimately, the production of CH<sub>3</sub>OH in present work was found to be competitive than previous works [30,31] illustrating the possibility of using ZnO/ZSM-5 composite in large scale applications for photocatalytic CO<sub>2</sub> conversion to methanol.

## 4. Conclusions

In this work, we presented ZnO incorporated in ZSM-5 prepared by wet-impregnation for photocatalytic CO<sub>2</sub> reduction into value-added chemicals. SEM analysis indicates good dispersion of nanometric ZnO onto external surface of ZSM-5. The FTIR and XRD results confirmed the phase formation of ZnO/ZSM-5. UV-Vis results revealed an obvious improvement in the absorbance of the UV-visible light region, while the bandgap of the modified ZnO was increased, as compared to the bare ZnO. The remarkable photocatalytic activity was exhibited for CH<sub>3</sub>OH generation (39.2 μmol/g.h) and HCOOH (0.72 μmol/g.h) by ZnO/ZSM-5 composite. These results demonstrated an alternative pathway for obtaining highly effective and low-cost catalyst to reach renewable solar fuels.

**Author Contributions:** Conceptualization, W.H.S., A.S., and I.D.M.B.; methodology, A.S., H.N.I., W.H.S.; formal analysis, H.S. and I.D.M.B.; investigation, I.D.M.B. and H.S.; resources, W.H.S.; data curation, A.S. and H.S.; writing—original draft preparation, A.S., H.N.I., H.S., and I.D.M.B.; writing—review and editing, A.S. and W.H.S.; visualization, A.S. and W.H.S.; supervision, W.H.S.; project administration, I.D.M.B.; funding acquisition, W.H.S., A.S., and I.D.M.B. All authors have read and agreed to the published version of the manuscript.

**Funding:** This research was funded by *Kementerian Pendidikan, Kebudayaan, Riset, dan Teknologi* (Grant No. 1949/E2/KM.05.01/2021) and *Penelitian Dasar Unggulan Perguruan Tinggi Kemendikbud/BRIN 2021* (1573A/IT1.C07.2/TA.00.2021).

**Acknowledgments:** The authors acknowledge the support from the Laboratory of Design Methodology, Process Design, and Control, Department of Chemical Engineering, Institut Teknologi Bandung.

**Conflicts of Interest:** The authors declare no conflict of interest.

## References

- Rodriguez, J.; Puzenat, E.; Thivel, P.-X. From solar photocatalysis to fuel-cell: A hydrogen supply chain. *J. Environ. Chem. Eng.* **2016**, *4*, 3001–3005.
- Mustafa, A.; Lougou, B. G.; Shuai, Y.; Wang, Z.; Tan, H. Current technology development for CO<sub>2</sub> utilization into solar fuels and chemicals: A review. *J. Energy Chem.* **2020**, *49*, 96–123.
- Ma, S.; Wang, W. Preparation and photocatalytic hydrogen evolution of g-C<sub>3</sub>N<sub>4</sub>/ZnO composite. *E3S Web Conf.* **2020**, *165*, 05007.
- Salazar, H.; Martins, P. M.; Santos, B.; Fernandes, M. M.; Reizabal, A.; Sebastián, V.; Botelho, G.; Tavares, C. J.; Vilas-Vilela, J. L.; Lanceros-Mendez, S. Photocatalytic and antimicrobial multifunctional nanocomposite membranes for emerging pollutants water treatment applications. *Chemosphere* **2020**, *250*, 126299.
- Theerthagiri, J.; Salla, S.; Senthil, R. A.; Nithyadharseni, P.; Madankumar, A.; Arunachalam, P.; Maiyalagan, T.; Kim, H.-S. A review on ZnO nanostructured materials: energy, environmental and biological applications. *Nanotechnology* **2019**, *30*, 392001.
- Kumaresan, N.; Ramamurthi, K.; Ramesh Babu, R.; Sethuraman, K.; Moorthy Babu, S. Hydrothermally grown ZnO nanoparticles for effective photocatalytic activity. *Appl. Surf. Sci.* **2017**, *418*, 138–146.
- Rai, S.; Bhujel, R.; Khadka, M.; Chetry, R. L.; Swain, B. P.; Biswas, J. Synthesis, characterizations, and electrochemical studies of ZnO/reduced graphene oxide nanohybrids for supercapacitor application. *Mater. Today Chem.* **2021**, *20*, 100472.
- Paul, R.; Kumbhakar, P.; Mitra, A. K. Blue–green luminescence by SWCNT/ZnO hybrid nanostructure synthesized by a simple chemical route. *Phys. E Low-dimensional Syst. Nanostructures* **2010**, *43*, 279–284.
- Zhao, L.; Ji, Y.; Sun, P.; Li, R.; Xiang, F.; Wang, H.; Ruiz-Martinez, J.; Yang, Y. Effects of individual and complex ciprofloxacin, fullerene C<sub>60</sub>, and ZnO nanoparticles on sludge digestion: Methane production, metabolism, and microbial community. *Bioresour. Technol.* **2018**, *267*, 46–53.
- Kumari, V.; Yadav, S.; Mittal, A.; Kumari, K.; Mari, B.; Kumar, N. Surface Plasmon response of Pd deposited ZnO/CuO nanostructures with enhanced photocatalytic efficacy towards the degradation of organic pollutants. *Inorg. Chem. Commun.* **2020**, *121*, 108241.
- Wang, C.; Shi, H.; Li, Y. Synthesis and characteristics of natural zeolite supported Fe<sup>3+</sup>-TiO<sub>2</sub> photocatalysts. *Appl. Surf. Sci.* **2011**, *257*, 6873–6877.
- Mohamed, R. M.; Mkhallid, I. A.; Abdel Salam, M.; Barakat, M. A. Zeolite Y from rice husk ash encapsulated with Ag-TiO<sub>2</sub>: characterization and applications for photocatalytic degradation catalysts. *Desalin. Water Treat.* **2013**, *51*, 7562–7569.
- Batistela, V. R.; Fogaça, L. Z.; Fávoro, S. L.; Caetano, W.; Fernandes-Machado, N. R. C.; Hioka, N. ZnO supported on zeolites: Photocatalyst design, microporosity and properties. *Colloids Surfaces A Physicochem. Eng. Asp.* **2017**, *513*, 20–27.
- Šuligoj, A.; Pavlović, J.; Arčon, I.; Rajić, N.; Novak Tušar, N. SnO<sub>2</sub>-Containing Clinoptilolite as a Composite Photocatalyst for Dyes Removal from Wastewater under Solar Light. *Catalysts* **2020**, *10*, 253.
- Zhang, W.; Wang, K.; Yu, Y.; He, H. TiO<sub>2</sub>/HZSM-5 nano-composite photocatalyst: HCl treatment of NaZSM-5 promotes photocatalytic degradation of methyl orange. *Chem. Eng. J.* **2010**, *163*, 62–67.
- TAKEUCHI, M.; KIMURA, T.; HIDAKA, M.; RAKHMAWATY, D.; ANPO, M. Photocatalytic oxidation of acetaldehyde with oxygen on TiO<sub>2</sub>/ZSM-5 photocatalysts: Effect of hydrophobicity of zeolites. *J. Catal.* **2007**, *246*, 235–240.
- Noorjahan, M. A novel and efficient photocatalyst: TiO<sub>2</sub>-HZSM-5 combine thin film. *Appl. Catal. B Environ.* **2004**, *47*, 209–213.
- Haghighi, M.; Rahmani, F.; Dehghani, R.; Tehrani, A. M.; Bagher Miranzadeh, M. Photocatalytic reduction of Cr (VI) in aqueous solution over ZnO/ HZSM-5 nanocomposite: Optimization of ZnO loading and process conditions. *Desalin. WATER Treat.* **2017**, *58*, 168–180.
- Khoshbin, R.; Haghighi, M. Direct syngas to DME as a clean fuel: The beneficial use of ultrasound for the preparation of CuO–ZnO–Al<sub>2</sub>O<sub>3</sub>/HZSM-5 nanocatalyst. *Chem. Eng. Res. Des.* **2013**, *91*, 1111–1122.
- Korkuna, O.; Lebeda, R.; Skubiszewska-Zięba, J.; Vrublevs'ka, T.; Gun'ko, V. M.; Ryczkowski, J. Structural and physicochemical properties of natural zeolites: clinoptilolite and mordenite. *Microporous Mesoporous Mater.* **2006**, *87*, 243–254.
- Khatamian, M.; Divband, B.; Jodaie, A. Degradation of 4-nitrophenol (4-NP) using ZnO nanoparticles supported on zeolites and modeling of experimental results by artificial neural networks. *Mater. Chem. Phys.* **2012**, *134*, 31–37.
- Flanigen, E. M. Chapter 2 Zeolites and molecular sieves: An historical perspective. In; 2001; pp. 11–35.
- Seijger, G. B. ; Oudshoorn, O. ; van Kooten, W. E. ; Jansen, J. ; van Bekkum, H.; van den Bleek, C. ; Calis, H. P. . In situ synthesis of binderless ZSM-5 zeolitic coatings on ceramic foam supports. *Microporous Mesoporous Mater.* **2000**, *39*, 195–204.

24. Song, C.; Li, X.; Zhu, X.; Liu, S.; Chen, F.; Liu, F.; Xu, L. Influence of the state of Zn species over Zn-ZSM-5/ZSM-11 on the coupling effects of cofeeding n-butane with methanol. *Appl. Catal. A Gen.* **2016**, *519*, 48–55.
25. Li, H.; Zhang, Y.; Diao, J.; Qiang, M.; Chen, Z. Synthesis and Photocatalytic Activity of Hierarchical Zn-ZSM-5 Structures. *Catalysts* **2021**, *11*, 797.
26. Wang, L.; Jin, P.; Duan, S.; She, H.; Huang, J.; Wang, Q. In-situ incorporation of Copper(II) porphyrin functionalized zirconium MOF and TiO<sub>2</sub> for efficient photocatalytic CO<sub>2</sub> reduction. *Sci. Bull.* **2019**, *64*, 926–933.
27. Shi, J.; Chen, J.; Feng, Z.; Chen, T.; Wang, X.; Ying, P.; Li, C. Time-Resolved Photoluminescence Characteristics of Subnanometer ZnO Clusters Confined in the Micropores of Zeolites. *J. Phys. Chem. B* **2006**, *110*, 25612–25618.
28. Flores, G.; Carrillo, J.; Luna, J. A.; Martínez, R.; Sierra-Fernandez, A.; Milosevic, O.; Rabanal, M. E. Synthesis, characterization and photocatalytic properties of nanostructured ZnO particles obtained by low temperature air-assisted-USP. *Adv. Powder Technol.* **2014**, *25*, 1435–1441.
29. Yaripour, F.; Shariatnia, Z.; Sahebdehfar, S.; Irandoukht, A. Conventional hydrothermal synthesis of nanostructured H-ZSM-5 catalysts using various templates for light olefins production from methanol. *J. Nat. Gas Sci. Eng.* **2015**, *22*, 260–269.
30. Luévano-Hipólito, E.; Torres-Martínez, L. M.; Fernández-Trujillo, A. Ternary ZnO/CuO/Zeolite composite obtained from volcanic ash for photocatalytic CO<sub>2</sub> reduction and H<sub>2</sub>O decomposition. *J. Phys. Chem. Solids* **2021**, *151*, 109917.
31. Huerta-Flores, A. M.; Luévano-Hipólito, E.; Torres-Martínez, L. M.; Torres-Sánchez, A. Photocatalytic H<sub>2</sub> production and CO<sub>2</sub> reduction on Cu, Ni-doped ZnO: effect of metal doping and oxygen vacancies. *J. Mater. Sci. Mater. Electron.* **2019**, *30*, 18506–18518.